IEEE Access
Multidisciplinary ⋮ Rapid Review ⋮ Open Access Journal

Received August 9, 2021, accepted August 19, 2021, date of publication August 24, 2021, date of current version August 30, 2021.

*Digital Object Identifier 10.1109/ACCESS.2021.3107033*

# Robust Neural Network Trajectory-Tracking Control of Underactuated Surface Vehicles Considering Uncertainties and Unmeasurable Velocities

**LANPING ZOU, HAITAO LIU, AND XUEHONG TIAN**
School of Mechanical and Power Engineering, Guangdong Ocean University, Zhanjiang 524088, China

Corresponding author: Xuehong Tian (gdtianxh@126.com)

This work was supported in part by the Natural Science Foundation of Guangdong Province in China under Grant 2018A0303130076, in part by the 2019 "Chong First-class" Provincial Financial Special Funds Construction Project under Grant 231419019, in part by the Science and Technology Planning Project of Zhanjiang City under Grant 2020B01267, and in part by the Fund of Southern Marine Science and Engineering Guangdong Laboratory (Zhanjiang) under Grant ZJW-2019-01.

**ABSTRACT** This article focuses on the trajectory-tracking of an underactuated surface vehicle (USV) considering model uncertainties and nonlinear environmental disturbances. For trajectory tracking in an actual USV sailing environment, both the inertia and damping matrixes are not diagonal, the velocities states are unmeasurable, and error constraints and input saturation are considered. A robust control strategy is proposed based on the backstepping method, state transformation, a super-twisting state observer, and neural networks. All the closed-loop signals are uniformly ultimately bounded, which is proved by the Lyapunov stability theory analysis. The advantages of the proposed method are as follows. (i) A super-twisting observer is constructed to solve the problem of the velocities being unmeasurable, and the error between the virtual and actual velocities converges to a small neighborhood around zero. (ii) Additional controllers are developed to address input saturation of the system control. (iii) A predefined function design is employed to guarantee the transient trajectory-tracking performance. Finally, simulation results verify the feasibility and effectiveness of the proposed USV trajectory-tracking control method.

**INDEX TERMS** Underactuated surface vehicle, trajectory tracking, prescribed performance, neural network, output feedback control.

## I. INTRODUCTION

Research on underactuated surface vessels (USVs) has developed rapidly over the past few decades, with growing exploration of and progress in marine science and technology. USVs are mainly used in two ways: for marine survey and defense, such as marine surveillance, disaster search and rescue, and coastal early warning [1], [2]. Examples of typical uses of USVs are the search of the wreckage of Malaysia Airlines M370 and conducting water depth and topographic surveys in Antarctica. Therefore, the design of advanced control strategies has been increasingly researched to accomplish these complex tasks more accurately in a real marine environment.

The associate editor coordinating the review of this manuscript and approving it for publication was Rongni Yang.

In current studies, USV control strategies include path-following control [3], [4], trajectory-tracking control [5], [6] and formation control [7], [8]. A path-following controller has no strict time requirements and is used to ensure USVs stably track a predefined reference path. In [3], finite-time path-tracking control and collision avoidance problems for USVs are solved in the presence of uncertainties and input saturation based on adaptive backstepping technique and the Lyapunov method. In [4], the good path-tracking performance is obtained by combining line-of-sight (LOS) and model predictive control (MPC) methods to improve the reference path-tracking precision. In [7], a distributed cooperative formation-tracking controller for fully automatic surface vessels is proposed based on a self-structured neural network to estimate the dynamics of unknown parameters, and an adaptive law is used to estimate unknown external

disturbances and the approximation errors of neural networks. In [8], a collision-avoiding and formation-tracking controller is proposed for USVs. The subject of this study is USV trajectory-tracking control. At present, a variety of nonlinear system control methods have been developed, such as backstepping control [9], [10], sliding mode control [11], [12], adaptive control [13], [14], robust $H\infty$ control [15], [16], neural network control [17], [18], and fuzzy control [19].

Model uncertainties and external disturbances are important system characteristics that cannot be neglected in designing algorithms for USV trajectory-tracking control [20], [21]. Many control methods have been used to address these issues. Among these methods, adaptive control is a widely applied control technology. In [22], a finite-time adaptive controller is designed considering input saturation. Although the controller considers environmental disturbances, model uncertainties are neglected. In [23], USV tracking performance is effectively improved by integrating an adaptive method with a sliding-mode disturbance observer. Neural network is an effective method with strong robustness that can be used to consider unknown complex uncertainties. In [24], neural networks (NNs) are used to approximate model uncertainties by introducing minimum learning parameters (MLPs) to reduce the computational complexity. However, the designed controller can only constrain the error signals to be semi-globally uniformly ultimate bounded (SGUUB). In [25], an adaptive radial basis function (RBF) NN is constructed to estimate a time-varying uncertain hydrodynamic damping term. However, it is assumed that the inertia matrix does not contain non-diagonal terms, which is not supported by the actual system model. In this study, complex unknown uncertainties are regarded as lumped uncertainties that are approximated using an RBF neural network and an adaptive law is designed to estimate the weights online.

In addition to uncertainties, we consider error constraints to improve transient and steady state performance, while enhancing the navigation safety of the USV system. Tracking errors that are not limited and go out of bounds can cause control failure. Predefining a performance function is an effective solution to solve the error constraint problem in most cases. In [26], predefined performance boundaries are extended to overcome problems with the convergence rate and maximum overshoot. In [27], USV trajectory tracking is stabilized using a predefined boundary constraint function that is time-varying and asymmetric. The used controller can make the tracking errors for the position and angle ultimately converge to a small neighborhood around zero. In [28], an error transformation method is presented that stabilizes tracking errors within a predetermined constraint boundary and improves tracking performance.

A variety of USV control methods can track a desired trajectory in the presence of complex uncertainties and error constraints. However, most of the studies that have been performed have used positive diagonal damping matrix and mass matrices, which are impractical. Fortunately, a coordinate transformation method has been proposed to solve the coupled problem by transforming the mass matrix into a diagonal form [29]. In [30], a state transformation method is developed to solve a coupled USV dynamic model. In [31], the aforementioned coordinate transformation method is used to investigate an adaptive output feedback controller for USV trajectory tracking. In [32], an adaptive USV trajectory-tracking controller is combined with a high-gain observer and a predefined performance function based on a realistic dynamical model.

USV velocities are unmeasurable in practice. In [33] and [34], a high-gain observer is used to obtain signals for immeasurable velocities. In [35], a novel super-twisting algorithm is designed to improve the tracking performance of a marine autonomous surface ship. In [36], a novel extended-states observer (ESO) is used to effectively estimate unmeasurable velocities. The field of under-driven control involves hybrid controllers, optimal control, fixed-time control, etc. In [37], a hybrid controller is used to determine absolute and relative speeds. In [38], an event-triggered scheme and a networked predictive control technique are proposed to stabilize networked control systems and save communication resources. In [39], a novel fixed-time control method is proposed to ensure fixed-time stability. In [40], a multi-objective optimization strategy is designed based on a nonlinear model predictive controller to reduce the number of adjustable control parameters. In [41], a finite-time extended state observer is established to improve the anti-interference ability and tracking accuracy of a USV system.

Considering the issues presented above, a USV trajectory-tracking control method is developed in this study to ensure tracking accuracy and transient performance under the conditions of unmeasurable velocities, input saturation, coupling and unknown lumped uncertainties. The main characteristics and contributions of this research study are described below.

(i): Unknown lumped uncertainties are estimated by RBF neural networks combined with an adaptive method.

(ii): The problem of unmeasurable velocities is addressed using a super-twisting observer.

(iii): The position error is constrained using a predefined performance function.

This article is structured as follows. In Section 2, the USV model, transformed error equations, and trajectory tracking control target are introduced. In Section 3, a USV trajectory-tracking controller is designed based on backstepping technique, a super-twisting observer, and neural networks. In Section 4, a stability proof based on Lyapunov stability theory is presented. In Section 5, the results of numerical simulations are presented to verify the effectiveness of the proposed controller. In Section 6, the conclusions are summarized.

## II. USV MODEL AND PROBLEM FORMULATION

In this section, the USV model, errors dynamics and control object are presented.

### A. MODEL DESCRIPTION

Herein, the USV kinematic and dynamic equations are presented. To derive a simple formula, we focus on the 3DOF (degrees of freedom) motion, with respect to the surge, sway and yaw axes.

The kinematics and dynamics of the multiple inputs and outputs of the USV can be described as follows:

$$\dot{\eta} = J(\phi)\upsilon \tag{1}$$

$$M\dot{\upsilon} + C(\upsilon)\upsilon + D(\upsilon)\upsilon = sat(\tau) + \tau_w \tag{2}$$

where

$$J(\phi) = \begin{bmatrix} \cos\phi & -\sin\phi & 0 \\ \sin\phi & \cos\phi & 0 \\ 0 & 0 & 1 \end{bmatrix}$$

and $\eta = [x, y, \phi]^T$ denotes the USV positions and orientations in the geodetic fixed frame. $\upsilon = [u, v, r]^T$ denotes the components of the surge, sway and yaw velocities. $M = M^T \in R^{3\times3}$ represents the non-diagonal positive-definite inertia matrix. $C(\upsilon) \in R^{3\times3}$ denotes the centripetal and Coriolis matrix. $D(\upsilon) \in R^{3\times3}$ denotes the damping matrix. $\tau_w = [\tau_{w1}, \tau_{w2}, \tau_{w3}]^T$ denotes the unknown bounded external disturbances. $J(\phi)$ is a nonsingular rotation matrix that is used to transform the coordinates from the body fixed frame (BFF) to the earth fixed frame (EFF). The term $sat(\tau) = [sat(\tau_u), 0, sat(\tau_r)]^T$ denotes the saturated control inputs, where the saturated error is given by $\Delta\tau = \tau - sat(\tau) = [\Delta\tau_u, 0, \Delta\tau_r]^T$.

$$sat(\tau_i) = \begin{cases} sign(\tau_i)\tau_{iM}, & |\tau_i| > \tau_{iM} \\ \tau_i, & |\tau_i| \le \tau_{iM}, \end{cases} \qquad i = u, r$$

where the upper bound $\tau_{iM}$ is known.

We streamline the controller design based on the kinematics and dynamic equations above by making the following assumptions.

*Assumption 1 ([42]):* The unmeasurable external perturbations $\tau_w$ are differentiable, time-varying and bounded. We can determine a positive constant $\bar{\tau}_w$ that satisfies $|\tau_w| \le \bar{\tau}_w$.

*Assumption 2 ([31])*: The reference trajectory $\eta_d = [x_d, y_d, \phi_d]^T$ is smooth, and its derivatives are bounded and smooth. The USV reference trajectory is given by $\dot{\eta}_d = J(\phi_d)\upsilon_d$.

*Remark 1:* In a practical ocean environment, the inertia matrix $M$ is time-varying and uncertain because of consumption and payload motion in the system. $C(\upsilon)$ and $D(\upsilon)$ cannot be estimated accurately.

To address this issue, $M$ is divided into a nominal part $M_n$ and an uncertain part $\Delta M$. It follows that $M = M_n + \Delta M$. Similarly, $C(\upsilon)$ and $D(\upsilon)$ are divided into nominal and uncertain dynamics. We thus obtain $C(\upsilon) = C_n(\upsilon) + \Delta C(\upsilon)$ and $D(\upsilon) = D_n(\upsilon) + \Delta D(\upsilon)$. The USV dynamics (2) can be expressed as

$$M_n\dot{\upsilon} + C_n(\upsilon)\upsilon + D_n(\upsilon)\upsilon = sat(\tau) + f \tag{3}$$

where $f = [f_1, f_2, f_3]^T = -\Delta M\dot{\upsilon} - \Delta C(\upsilon)\upsilon - \Delta D(\upsilon)\upsilon + \tau_w$.

$$D_n(\upsilon) = \begin{bmatrix} d_{11}(\upsilon) & 0 & 0 \\ 0 & d_{22}(\upsilon) & d_{23}(\upsilon) \\ 0 & d_{32}(\upsilon) & d_{33}(\upsilon) \end{bmatrix},$$

$$M_n = \begin{bmatrix} m_{11} & 0 & 0 \\ 0 & m_{22} & m_{23} \\ 0 & m_{32} & m_{33} \end{bmatrix},$$

$$C_n(\upsilon) = \begin{bmatrix} 0 & 0 & c_{13}(\upsilon) \\ 0 & 0 & c_{23}(\upsilon) \\ c_{31}(\upsilon) & c_{32}(\upsilon) & 0 \end{bmatrix}.$$

### B. COORDINATE TRANSFORMATION

The USV inertia matrix is coupled, that is, the yaw moment $\tau_r$ acts on both the yaw and sway axes. Thus, it is difficult to design a controller and analyze the tracking performance directly.

To solve this problem, we adopt the following state transformation method [30]:

$$\bar{x} = x + \delta\cos\phi, \quad \bar{y} = y + \delta\sin\phi, \quad \bar{v} = v + \delta r \tag{4}$$

where $\delta = m_{23}/m_{22}$. This transformation is equivalent to moving the body frame origin by a small distance $\delta$ in the surge motion direction.

Let $\bar{\eta} = [\bar{x}, \bar{y}, \phi]^T$ and $\bar{\upsilon} = [u, \bar{v}, r]^T$; the USV dynamics given in (3) can then be rewritten as

$$\dot{\bar{\eta}} = J(\phi)\bar{\upsilon} \tag{5}$$

$$\dot{\bar{\upsilon}} = \vartheta + F + \bar{\tau} \tag{6}$$

where $F = [F_1, F_2, F_3]^T = [f_1/m_{11}, f_2/m_{22}, (-m_{23}f_2 + m_{22}f_3)/\Upsilon]^T$,

$\bar{\tau} = [(\tau_u + \Delta\tau_u)/m_{11}, 0, m_{22}(\tau_r + \Delta\tau_u)/\Upsilon]^T$,

$\vartheta = [\vartheta_1, \vartheta_2, \vartheta_3]^T$ and $\Upsilon = m_{22}m_{33} - m_{23}^2$. Here, the expression for the vector $\vartheta$ is

$$\begin{aligned} \vartheta_1 &= (m_{22}(\bar{v} - \delta r)r + m_{23}r^2 - d_{11}u)/m_{11} \\ \vartheta_2 &= (-m_{11}ur - d_{22}(\bar{v} - \delta r) - d_{23}r)/m_{22} \\ \vartheta_3 &= ((m_{11}m_{22} - m_{22}^2)u(\bar{v} - \delta r) + (m_{11}m_{23} - m_{22}m_{23})ur \\ &\quad -(d_{33}r + d_{32}(\bar{v} - \delta r))m_{22} \\ &\quad + (d_{23}r + d_{22}(\bar{v} - \delta r))m_{23})/\Upsilon \end{aligned} \tag{7}$$

### C. ERROR DYNAMICS OF TRAJECTORY TRACKING

To present the problem formulation more clearly, the relations between the USV BFF and the EFF are shown in FIGURE 1.

In the figure, $O_b - X_bY_bZ_b$ is the USV body-fixed frame, and $O - XYZ$ is the earth-fixed inertial frame.

The USV tracking errors are defined as

$$x_e = \bar{x} - \bar{x}_d, y_e = \bar{y} - \bar{y}_d, \phi_e = \phi - \phi_c \tag{8}$$

where $\bar{x}_d = x_d + \delta\cos\phi_d$, $\bar{y}_d = y_d + \delta\sin\phi_d$, and $\phi_c$ denote the desired azimuth angle related to $\phi_d, x_e, y_e$ as

$$\phi_c = \arctan\frac{y_e}{x_e}\tanh(E^2/c) + \phi_d(1 - \tanh(E^2/c)) \tag{9}$$

where $E = \sqrt{x_e^2 + y_e^2}$ and $c$ is a positive constant.

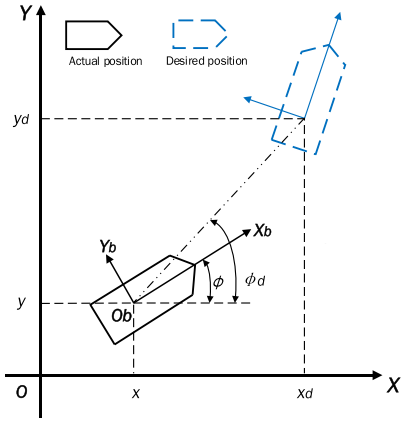


**FIGURE 1.** Navigation and body frames for USV trajectory tracking.

Differentiating both sides of (8) yields

$$\begin{aligned}\dot{x}_e &= u\cos\phi - \bar{v}\sin\phi - \dot{\bar{x}}_d \\ \dot{y}_e &= u\sin\phi + \bar{v}\cos\phi - \dot{\bar{y}}_d \\ \dot{\phi}_e &= r - \dot{\phi}_c\end{aligned} \tag{10}$$

This paper aims to design the control force $\tau_u$ and torques $\tau_r$ based on output feedback to constrain the USV trajectory-tracking errors and velocity-tracking errors within predefined bounds.

## III. CONTROLLER DESIGN

In this section, the design of a dynamic output feedback controller based on the backstepping method and RBF neural networks (NNs) is presented.

### A. NEURAL NETWORKS

As for system (6), we use RBF NNs to approximate the lumped nonlinear uncertainties $F_1, F_2, F_3$. The results can be expressed as [43]

$$\begin{aligned}F(X_j) &= W_j^{*T}\Theta(X_j) + \zeta_j^* \\ W^* &= \arg\min[\sup\left|F(X) - \hat{F}(X,\hat{W})\right|]\end{aligned} \tag{11}$$

where $j = 1, 2, 3. W_j^* \in R^n$ is the optimal weight. $\zeta_j^*$ is the bounded approximation error, where $\left|\zeta_j^*\right| \le \bar{\zeta}$. $\Theta(X_j) = [\Theta_{j,1}, \Theta_{j,2}, \ldots, \Theta_{j,n}]^T$ denotes the Gaussian basis function:

$$\Theta(X_j) = \exp(-\frac{\left\|X_j - c_j\right\|}{b_j^2}), \quad j = 1, 2, \cdots, n \tag{12}$$

where $n$ is the number of RBF NNs nodes. $c_j$ and $b_j$ are the center and width of the basis function, respectively.

The RBF NNs have the following properties:

$$-h_i\tilde{W}_i^T\hat{W}_i \le \frac{h_i}{2}\left(\left\|W_i^*\right\|^2 - \left\|\tilde{W}_i\right\|^2\right), \quad i = 1, 2, 3. \tag{13}$$

### B. SUPER-TWISTING VELOCITY OBSERVER

The immeasurability of the velocity states is addressed in this subsection.

Let $\hat{x}, \hat{y}, \hat{\phi}, \hat{u}, \hat{v}, \hat{r}$ represent the estimated values of $\bar{x}, \bar{y}, \phi, u, \bar{v}, r$, respectively.

It is well known that $\dot{J}(\phi) = J(\phi)S(r)$, where $S(r) = \begin{bmatrix} 0 & -r & 0 \\ r & 0 & 0 \\ 0 & 0 & 0 \end{bmatrix}$.

The coordinate transformation on $\bar{\vartheta}$, $w = J(\phi)\bar{\vartheta} = [w_1, w_2, w_3]^T$ yields

$$\begin{cases}\dot{\bar{\eta}} = w \\ \dot{w} = g(t, \bar{\eta}, w, \tau) + \xi(t, \bar{\eta}, w, \tau)\end{cases} \tag{14}$$

where $g(t, \bar{\eta}, w, \tau) = S(r)w + J(\phi)\vartheta + J(\phi)\bar{\tau}$ represents the nominal part of the USV system dynamics. $\xi(t, \bar{\eta}, w, \tau) = J(\phi)F$ are the uncertainties.

Inspired by [44], a STA observer is designed to solve the problem of the unmeasurable velocity based on the characteristics of the USV system dynamics. The model (11) is rewritten in state-space form as follows:

$$\begin{cases}\dot{\hat{\eta}} = w + z_1 \\ \dot{\hat{w}} = g(t, \eta, \hat{w}, \tau) + z_2\end{cases} \tag{15}$$

where $\hat{\eta}$ and $\hat{w}$ are the state estimates, $z_1$ and $z_2$ are correction variables with the following form:

$$\begin{cases}z_1 = \lambda\left|\bar{\eta} - \hat{\eta}\right|^{1/2} sign\left(\bar{\eta} - \hat{\eta}\right) \\ z_2 = \alpha sign\left(\bar{\eta} - \hat{\eta}\right)\end{cases} \tag{16}$$

Thus, the unmeasurable velocity $\vartheta$ can be estimated as

$$\hat{\upsilon} = J^T(\hat{w} + z_1) \tag{17}$$

The velocity observed errors are defined as

$$u_e = \hat{u} - u \quad v_e = \hat{v} - \bar{v} \quad r_e = \hat{r} - r \tag{18}$$

The proposed super-twisting velocity observer is used to accurately observe the velocities. Thus, these velocities can be considered as known information. The following notation is used in Section IV: $\hat{u} \equiv u, \hat{v} \equiv \bar{v}, \hat{r} \equiv r$.

### C. POSITION-TRANSFORMED ERROR CONTROL

In this subsection, the position tracking errors in (8) are guaranteed to converge by using a predefined bounded performance function and the backstepping method.

*Definition 1:* A smooth function $\beta(t)$ is a predefined bound performance function [45] if $\beta(t)$ is positive and monotonically decreasing, where $\lim_{t\to\infty}\beta(t) = \beta_\infty > 0$. This function is expressed as

$$\beta(t) = (\beta_0 - \beta_\infty)e^{-kt} + \beta_\infty \tag{19}$$

where $\beta_0$, $\beta_\infty$, $\alpha$ are positive scale constants. $\beta_0$ and $\beta_\infty$ determine the overshoot and steady-state performance, respectively, and $k$ represents a suitable predefined convergence rate. To guarantee the predefined performance, we set

$$-\beta_1(t) < x_e(t) < \beta_1(t)$$

$$-\beta_2(t) < y_e(t) < \beta_2(t)$$
$$-\beta_3(t) < \phi_e(t) < \beta_3(t) \tag{20}$$

To ensure effective constrained trajectory-tracking performance, the conversion errors are defined as

$$e_x = \Lambda(\frac{x_e}{\beta_1}) \quad e_y = \Lambda(\frac{y_e}{\beta_2}) \quad e_\varphi = \Lambda(\frac{\phi_e}{\beta_3}) \tag{21}$$

Setting $z_1 = \frac{x_e}{\beta_1}, z_2 = \frac{y_e}{\beta_2}, z_3 = \frac{\phi_e}{\beta_3}$ yields

$$\Lambda(z_i) = \ln(\frac{1+z_i}{1-z_i}), \quad i = x, y, \phi \tag{22}$$

Differentiating both sides of (21) yields

$$\dot{e}_x = \frac{2(\beta_1\dot{x}_e - x_e\dot{\beta}_1)}{(1-z_1^2)\beta_1^2}, \quad \dot{e}_y = \frac{2(\beta_2\dot{y}_e - y_e\dot{\beta}_2)}{(1-z_2^2)\beta_2^2}$$
$$\dot{e}_\phi = \frac{2(\beta_3\dot{\phi}_e - \phi_e\dot{\beta}_3)}{(1-z_3^2)\beta_3^2} \tag{23}$$

*Remark 2*: We define the mapping relation $\Lambda(\cdot) : (-1, 1) \to (-\infty, \infty), \Lambda(0) = 0.\Lambda(z_i)$ is a smooth and strictly increasing function.

*Remark 3*: We choose appropriate control parameters such that if the transformed error $e_x, e_y, e_\phi$ are bounded, then $x_e, y_e, \phi_e$ are bounded and steady.

To stabilize the trajectory tracking position errors, we define $g_i = (1-z_i^2)\beta_i, i = 1, 2, 3$, and choose a Lyapunov function as

$$V_1 = \frac{1}{2}g_1e_x^2 + \frac{1}{2}g_2e_y^2 + \frac{1}{2}g_3e_\phi^2 \tag{24}$$

### D. VIRTUAL VELOCITY DESIGN

In this subsection, we design appropriate virtual velocities $\upsilon_f = [u_f, v_f, r_f]^T$ to stabilize the position transformed errors $e_x$, $e_y$ and $e_\phi$. The virtual velocities $\upsilon_f = [u_f, v_f, r_f]^T$ are designed as

$$u_f = -\lambda_1 e_x\cos\phi - \lambda_1 e_y\sin\phi + \dot{\bar{x}}_d\cos\phi + \dot{\bar{y}}_d\sin\phi$$
$$v_f = \lambda_1 e_x\sin\phi - \lambda_1 e_y\cos\phi - \dot{\bar{x}}_d\sin\phi + \dot{\bar{y}}_d\cos\phi$$
$$r_f = -\lambda_2 e_\phi + \dot{\phi}_d \tag{25}$$

Combining (15) and (25) yields the errors between the virtual and transformed velocities as

$$s_1 = u - u_f - \alpha_1\tanh\rho_1$$
$$s_2 = \bar{v} - v_f - \alpha_2\tanh\rho_2$$
$$s_3 = r - r_f - \alpha_3\tanh\rho_3 \tag{26}$$

where $\alpha_1, \alpha_2, \alpha_3$ are positive constants. $\rho_1, \rho_2, \rho_3$ are designed as

$$\dot{\rho}_1 = \cosh^2\rho_1(-\mu_u\rho_1 - \Delta\tau_u/m_{11})/\alpha_1$$
$$\dot{\rho}_2 = \cosh^2\rho_2(\hat{W}_2^T\Theta_2\left(\hat{X}\right) - \lambda_3 s_1 + \lambda_3 s_2 - \lambda_3 s_3 + \xi_2)/\alpha_2$$
$$\dot{\rho}_3 = \cosh^2\rho_3(-\mu_r\rho_3 - m_{22}\Delta\tau_u/\Upsilon)/\alpha_3 \tag{27}$$

where $\lambda_3, \mu_u, \mu_r$ are positive constants.

Substituting (26) into (10) yields

$$\dot{x}_e = (s_1 + u_f + \alpha_1\tanh\rho_1)\cos\phi - (s_2 + v_f + \alpha_2\tanh\rho_2)\sin\phi - \dot{\bar{x}}_d$$
$$\dot{y}_e = (s_1 + u_f + \alpha_1\tanh\rho_1)\sin\phi + (s_2 + v_f + \alpha_2\tanh\rho_2)\cos\phi - \dot{\bar{y}}_d$$
$$\dot{\phi}_e = (s_3 + r_f + \alpha_3\tanh\rho_3) - \dot{\phi}_c \tag{28}$$

Substituting (28) into (23) yields

$$\dot{e}_x = (-2\lambda_1 e_x + 2s_1\cos\phi - 2s_2\sin\phi + \psi_1)/g_1$$
$$\dot{e}_y = (-2\lambda_1 e_y + 2s_1\sin\phi + 2s_2\cos\phi + \psi_2)/g_2$$
$$\dot{e}_\phi = (-2\lambda_2 e_\phi + 2s_3 + \psi_3)/g_3 \tag{29}$$

where $g_i = (1-z_i^2)\beta_i, i = 1, 2, 3,$

$$\psi_1 = 2\alpha_1\cos\phi\tanh\rho_1 - 2\alpha_2\sin\phi\tanh\rho_2 - 2\dot{\beta}_1 z_1,$$
$$\psi_2 = 2\alpha_1\sin\phi\tanh\rho_1 + 2\alpha_2\cos\phi\tanh\rho_2 - 2z_2\dot{\beta}_2,$$
$$\psi_3 = 2\alpha_3\tanh\rho_3 - 2\dot{\phi}_c + 2\dot{\phi}_d - 2z_3\dot{\beta}_3.$$

*Remark 4*: $\dot{\bar{x}}_d, \dot{\bar{y}}_d, \dot{\phi}_c$ are available and bounded. Using $|\sin(\cdot)| \le 1, |\cos(\cdot)| \le 1, |\tanh(\cdot)| \le 1$ in conjunction with (19) and (22) yields $\left|\Lambda^{-1}(\cdot)\right| \le 1, |\beta_i| \le \alpha_i(\beta_{i,0} - \beta_{i,\infty}), i = 1, 2, 3$. Thus, it is proven that positive constants $\bar{\psi}_i, \bar{g}_i$ exist that satisfy $\psi_i \le \bar{\psi}_i, g_i \le \beta_{i,0}, \dot{g}_i \le \bar{g}_i, i = 1, 2, 3$.

Differentiating (26) and combining the result with (27) yields

$$\dot{s}_1 = \dot{u} - \dot{u}_f + \mu_u\rho_1 + \Delta\tau_u/m_{11}$$
$$\dot{s}_2 = \dot{\bar{v}} - \dot{v}_f - \hat{W}_2^T\Theta_2(\hat{X}) + \lambda_3 s_1 - \lambda_3 s_2 + \lambda_3 s_3 - \vartheta_2$$
$$\dot{s}_3 = \dot{r} - \dot{r}_f + \mu_r\rho_3 + m_{22}\Delta\tau_r/\Upsilon \tag{30}$$

Combining the definitions $\tau_u = \Delta\tau_u + sat(\tau_u)$ and $\tau_r = \Delta\tau_r + sat(\tau_r)$ with (30) yields

$$\dot{s}_1 = \vartheta_1 + F_1 - \dot{u}_f + \mu_u\rho_1 + \tau_u/m_{11}$$
$$\dot{s}_2 = F_2 - \dot{v}_f - \hat{W}_2^T\Theta_2(X) + \lambda_3 s_1 - \lambda_3 s_2 + \lambda_3 s_3$$
$$\dot{s}_3 = \vartheta_3 + F_3 - \dot{r}_f + \mu_r\rho_3 + m_{22}\tau_r/\Upsilon \tag{31}$$

where $X = [s_1, s_2, s_3, x_e, y_e, \phi_e]^T$.

Therefore, we design an output feedback control law for $\tau_u, \tau_r$ and an adaptive law for $\hat{W}$ as

$$\tau_u = m_{11}(-\lambda_3 s_1 - \lambda_3 s_2 - \hat{W}_1^T\Theta_1(\hat{X}) - \hat{\vartheta}_1 - \mu_u\rho_1)$$
$$\tau_r = \Upsilon(-\lambda_3 s_2 - \lambda_3 s_3 - \hat{W}_3^T\Theta_3(\hat{X}) - \hat{\vartheta}_3 - \mu_r\rho_3)/m_{22}$$
$$\dot{\hat{W}} = \Gamma_i(\Theta_i(\hat{X})s - h_i\hat{W}_i), \quad i = 1, 2, 3 \tag{32}$$

where $h_i > 0$.

Substituting (32) into (31) yields

$$\dot{s}_1 = -\lambda_3 s_1 - \lambda_3 s_2 + F_1 - \vartheta_1 - \dot{u}_f - \hat{W}_1^T\Theta_1(\hat{X})$$
$$\dot{s}_2 = \lambda_3 s_1 - \lambda_3 s_2 + \lambda_3 s_3 - \vartheta_2 + F_2 - \dot{v}_f - \hat{W}_2^T\Theta_2(\hat{X})$$
$$\dot{s}_3 = -\lambda_3 s_2 - \lambda_3 s_3 + F_3 - \vartheta_3 - \dot{r}_f - \hat{W}_3^T\Theta_3(\hat{X}) \tag{33}$$

where $\tilde{\xi}_1 = \hat{\xi}_1 - \xi_1, \tilde{\xi}_2 = \hat{\xi}_2 - \xi_2, \tilde{\xi}_3 = \hat{\xi}_3 - \xi_3$.

Defining $\sigma_1 = F_1 - \dot{u}_f - W_1^{*T}\Theta_1(X)$, $\sigma_2 = F_2 - \dot{v}_f - W_2^{*T}\Theta_2(X)$ and $\sigma_3 = F_3 - \dot{r}_f - W_3^{*T}\Theta_3(X)$ yields

$$\begin{aligned}\dot{s}_1 &= -\lambda_3 s_1 - \lambda_3 s_2 - \vartheta_1 + W_1^{*T}\Theta_1(X) - \hat{W}_1^T\Theta_1(\hat{X}) + \sigma_1\\ \dot{s}_2 &= \lambda_3 s_1 - \lambda_3 s_2 + \lambda_3 s_3 - \vartheta_2 + W_2^{*T}\Theta_2(X) - \hat{W}_2^T\Theta_2(\hat{X}) + \sigma_2\\ \dot{s}_3 &= -\lambda_3 s_2 - \lambda_3 s_3 - \vartheta_3 + W_3^{*T}\Theta_3(X) - \hat{W}_3^T\Theta_3(\hat{X}) + \sigma_3\end{aligned} \tag{34}$$

Let us define a new Lyapunov function as

$$V_2 = \frac{1}{2}s_1^2 + \frac{1}{2}s_2^2 + \frac{1}{2}s_3^2 \tag{35}$$

$$V_3 = \sum_{i=1}^{3}\tilde{W}_i^T\Gamma_i^{-1}\tilde{W}_i \tag{36}$$

## IV. STABLITY ANALYSIS OF USV SYSTEM

*Theorem 1:* For the USV system with kinematics (1) and dynamics (2), under the velocity states observer, the virtual velocity laws (25), and the control laws (32), appropriate control parameters $\alpha_1, \alpha_2, \alpha_3, l_1, l_2, l_3, \lambda_1, \lambda_2, \lambda_3$ exist such that the USV control system states are bounded and converge to a predefined scope.

A Lyapunov function candidate is constructed as

$$V = V_1 + V_2 + V_3 \tag{37}$$

*Remark 5*: Suitable parameters $\beta_{1,0}$, $\beta_{2,0}$, $\beta_{3,0}$ are chosen to ensure that the initial transformed tracking errors are bounded, that is, $|e_x(0)| < \beta_{1,0}$, $|e_y(0)| < \beta_{2,0}$, $|e_\phi(0)| < \beta_{3,0}$. Then, the following conclusion can be drawn: the error converges to a small range around zero, and the closed-loop USV system states are ultimately bounded.

Substituting (29) into the expressions for the time derivatives of $V_1$ given in (24) yields

$$\begin{aligned}\dot{V}_1 &= g_1 e_x\dot{e}_x + g_2 e_y\dot{e}_y + g_3 e_\phi\dot{e}_\phi\\ &\quad + e_x^2\dot{g}_1/2 + e_y^2\dot{g}_2/2 + e_\phi^2\dot{g}_3/2\\ &= -2\lambda_1 e_x^2 - 2\lambda_2 e_y^2 - 2\lambda_2 e_\phi^2 + 2e_x(s_1\cos\phi - s_2\sin\phi)\\ &\quad + 2e_y(s_1\sin\phi + s_2\cos\phi) + 2e_\phi s_3 + e_x\psi_1 + e_y\psi_2\\ &\quad + e_\phi\psi_3 + e_x^2\dot{g}_1/2 + e_y^2\dot{g}_2/2 + e_\phi^2\dot{g}_3/2\end{aligned} \tag{38}$$

Then, applying Young's inequality yields $\dot{V}_1$ as

$$\begin{aligned}\dot{V}_1 \le &-(2\lambda_1 - \bar{g}_1/2 - 5/2)e_x^2 - (2\lambda_1 - \bar{g}_2/2 - 5/2)e_y^2\\ &-(2\lambda_1 - \bar{g}_3/2 - 3/2)e_\phi^2 + 2\sum_{i=1}^{3}s_i^2 + \frac{1}{2}\sum_{i=1}^{3}\bar{\psi}_i^2\end{aligned} \tag{39}$$

Substituting (34) into the time derivatives of $V_2$ given in (35) yields

$$\begin{aligned}&\dot{V}_2\\ &= s_1(-\lambda_3 s_1 - \lambda_3 s_2 - \tilde{\xi}_1 + W_1^{*T}\Theta_1(X) - \hat{W}_1^T\Theta_1(\hat{X}) + \sigma_1)\\ &\quad + \hat{s}_2(\lambda_3 s_1 - \lambda_3 s_2 + \lambda_3 s_3 - \tilde{\xi}_2 + W_2^{*T}\Theta_2(X)\\ &\quad - \hat{W}_2^T\Theta_2(\hat{X}) + \sigma_2)\\ &\quad + s_2(-\lambda_3 s_2 - \lambda_3 s_3 - \tilde{\xi}_3 + W_3^{*T}\Theta_3(X) - \hat{W}_3^T\Theta_3(\hat{X}) + \sigma_3)\\ &= -\lambda_3\sum_{i=1}^{3}s_i^2 + \sum_{i=1}^{3}s_i(W_i^{*T}\Theta_i(X) - \hat{W}_i^T\Theta_i(\hat{X}) + \sigma_i)\\ &\quad - \sum_{i=1}^{3}s_i\tilde{\xi}_i\end{aligned} \tag{40}$$

Substituting the adaptive law (32) into the expressions for the time derivatives of $V_3$ given in (36) yields

$$\dot{V}_3 = \sum_{i=1}^{3}(\tilde{W}_i^T\Theta_i(\hat{X})s_i - h_i\tilde{W}_i^T\hat{W}_i) \tag{41}$$

Considering the RBF NNs properties given by (13) yields

$$\dot{V}_3 \le \sum_{i=1}^{3}(\tilde{W}_i^T\Theta_i(\hat{X})s_i + \frac{h_i}{2}\left\|W_i^*\right\|^2 - \frac{h_i}{2}\left\|\tilde{W}_i\right\|^2) \tag{42}$$

Considering (39), (40), and (42), and taking the time derivatives of the expression for $V$ given in (37) yields

$$\begin{aligned}\dot{V} \le &-(2\lambda_1 - \bar{g}_1/2 - 5/2)e_x^2 - (2\lambda_1 - \bar{g}_2/2 - 5/2)e_y^2\\ &-(2\lambda_1 - \bar{g}_3/2 - 3/2)e_\phi^2 + (2-\lambda_3)\sum_{i=1}^{3}s_i^2 - \sum_{i=1}^{3}\tilde{\xi}_i s_i\\ &+\sum_{i=1}^{3}s_i\sigma_i + \frac{1}{2}\sum_{i=1}^{3}\bar{\psi}_i^2 + \sum_{i=1}^{3}\frac{h_i}{2}\left\|W_i^*\right\|^2 - \sum_{i=1}^{3}\frac{h_i}{2}\left\|\tilde{W}_i\right\|^2\\ &+\sum_{i=1}^{3}(s_i W_i^{*T}\Theta_i(X) - s_i\hat{W}_i^T\Theta_i(\hat{X}) + \tilde{W}_i^T\Theta_i(\hat{X})s_i)\end{aligned} \tag{43}$$

*Remark 6*: The terms $\vartheta_i, i = 1, 2, 3$ given in (6) are expressed with respect to $\upsilon$. We design the control inputs considering saturation to ensure that the velocities $\upsilon = [u, v, r]^T$ are bounded. Finally, we assume that $\xi_1, \xi_2, \xi_3$ are Lipschitz functions.

Using the aforementioned assumptions yields the inequalities $\sum_{i=1}^{3}\tilde{\xi}_i s_i \le \sum_{i=1}^{3}(q_i s_i^2 + q_4)$, where $q_1, q_2, q_3, q_4$ are positive constants.

To simplify $\dot{V}$ in (43), we use the following inequality:

$$\begin{aligned}-W_i^{*T}\Theta_i(X) + \hat{W}_i^T\Theta_i(\hat{X}) &= \tilde{W}_i^T\Theta_i(\hat{X})\\ &\quad + W_i^{*T}(\Theta_i(X) - \Theta_i(\hat{X}))\\ &\le \tilde{W}_i^T\Theta_i(\hat{X}) + \varepsilon_i\left\|W_i^*\right\|\end{aligned} \tag{44}$$

Combining this result with the previous inequality yields

$$\begin{aligned}\dot{V} \le &-(2\lambda_1 - \bar{g}_1/2 - 5/2)e_x^2 - (2\lambda_1 - \bar{g}_2/2 - 5/2)e_y^2\\ &-(2\lambda_1 - \bar{g}_3/2 - 3/2)e_\phi^2 - (-3 + \lambda_3 - q_1)s_1^2\\ &-(-3 + \lambda_3 - q_2)s_2^2 - (-3 + \lambda_3 - q_3)s_3^2\\ &+\frac{1}{2}(\sum_{i=1}^{3}\bar{\psi}_i^2 + \sum_{i=1}^{3}(h_i + \varepsilon_i^2)\left\|W_i^*\right\|^2 + \sum_{i=1}^{3}\bar{\sigma}_i^2)\end{aligned} \tag{45}$$

Let us define $D$, $\mu$ as

$$D = \frac{1}{2}(\sum_{i=1}^{3}\bar{\psi}_i^2 + \sum_{i=1}^{3}(h_i + \varepsilon_i^2)\left\|W_i^*\right\|^2 + \sum_{i=1}^{3}\bar{\sigma}_i^2) \tag{46}$$

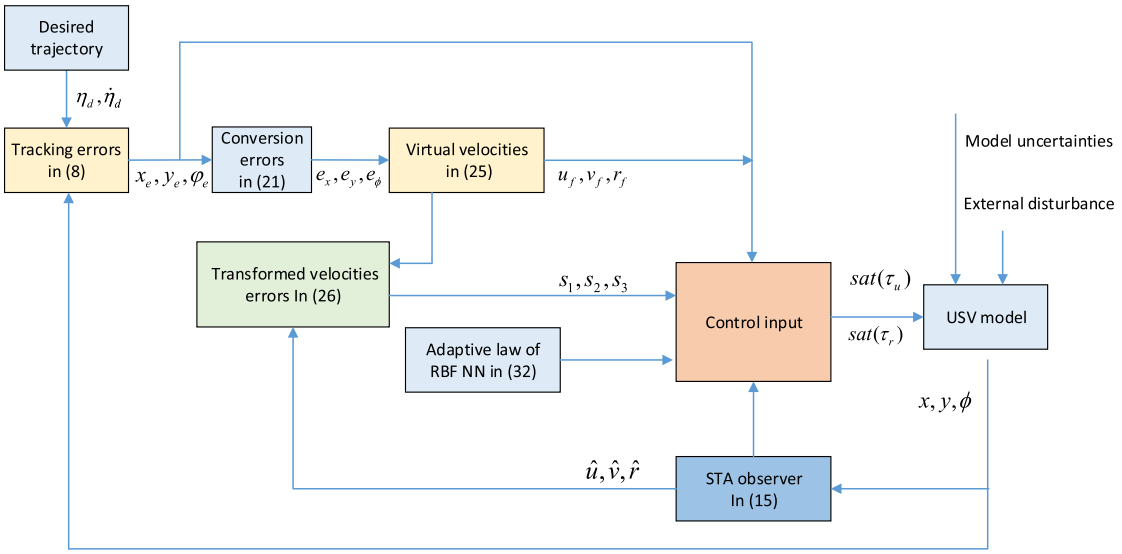


**FIGURE 2.** The architecture of the control method for to an underactuated surface vessel.

$$\mu = \min\left(\frac{2\lambda_1 - \bar{g}_1/2 - 5/2}{\beta_{1,0}}, \frac{2\lambda_1 - \bar{g}_2/2 - 5/2}{\beta_{2,0}}, \frac{2\lambda_2 - \bar{g}_3/2 - 3/2}{\beta_{3,0}}, -3 + \lambda_3 - q_1, -3 + \lambda_3 - q_2, -3 + \lambda_3 - q_3, \min\left(\frac{h_i}{\lambda_{\max}(\Gamma_i^{-1})}\right)\right) \tag{47}$$

The following suitable control parameters are chosen to ensure that $\mu$ is always a positive constant.

$$\begin{aligned} \lambda_1 &\geq \max(\bar{g}_1/4 + 5/4, \bar{g}_2/4 + 5/4, \bar{g}_3/4 + 3/4) \\ \lambda_2 &\geq \bar{g}_3/4 + 3/4 \\ \lambda_3 &\geq \max(3 + q_1, 3 + q_2, 3 + q_3) \end{aligned} \tag{48}$$

Then, substituting (46) and (47) into (45) yields

$$\dot{V} \leq -\mu V + D \tag{49}$$

Solve the above equation (49), yields

$$V(t) \leq (V(0) - D/\mu)\, e^{-\mu t} + D/\mu \tag{50}$$

Finally, we conclude that the USV closed-loop system is stable and that the transformed errors $e_x, e_y, e_\phi$ in (21) are bounded. The coordinate transformation method given in (4) is equivalent to moving the origin of the BFF to the EFF forward by a very small distance $\delta$ along the surge direction. Thus, the transformed errors are essentially the same as the errors in the original coordinates. Thus, the original errors are also bounded. The proposed control architecture is shown in FIGURE 2.

## V. SIMULATIONS AND COMPARATIVE ANALYSIS

In the section, the procedure for numerical simulations used to analyze the performance of the proposed controller is presented. The trajectory-tracking efficiency of the designed controller is verified using the USV model parameters in [29]:

$$\begin{aligned} m_{11} &= 141.85, m_{22} = 191.75, m_{23} = 5.7, m_{32} = 5.7, \\ m_{33} &= 15.6, c_{13}(\upsilon) = -191.75v - 5.7r, \\ c_{23}(\upsilon) &= 141.85u, c_{31}(\upsilon) = 191.75v \\ &\quad +5.7r, c_{32}(\upsilon) = -141.85u, \\ d_{11}(\upsilon) &= 45.6 + 67.26\,|u| + 10u^2, \\ d_{22}(\upsilon) &= 29.54 + 73.85\,|v| + 15\,|r|, \\ d_{23}(\upsilon) &= -2.5 + 2\,|v| + 10.71\,|r|, \\ d_{32}(\upsilon) &= -2.4 - 13\,|v| - 0.2\,|r|, \\ d_{33}(\upsilon) &= 5.59 + 10.71\,|v| - 0.07\,|r|. \end{aligned}$$

First, as in [10], the USV reference trajectory is assumed to be

$$y_d = \begin{cases} 2.1\sin(\pi t/75), & 0 < t < 37.5 \\ 2.1, & t < 112.5 \\ -2.1\sin(\pi t/75), & t < 187.5 \\ -2.1, & t >= 187.5 \end{cases}$$

$$x_d = 0.9t, \quad \phi_d = arc\tan\left(\frac{\dot{y}_d}{\dot{x}_d}\right) \tag{51}$$

The USV initial conditions of USV are selected as

$$\begin{aligned} &x(0) = 0.5m, \quad y(0) = 0.5m, \ \phi(0) = 0rad, \\ &u(0) = 0.3m/s, \quad v(0) = 0.1m/s, \ r(0) = 0rad/s. \end{aligned} \tag{52}$$

To verify the performance of the designed controller, we add an external disturbance from [24] and the following external time-varying disturbances:

$$\tau_w = \begin{bmatrix} -8 + 1.2\sin(0.05t) + 1.8\sin(0.7t) + 1.2\sin(0.05t) \\ 0.2\cos(0.5t) - 4 + 0.4\sin(0.1t) \\ 0 \end{bmatrix} \tag{53}$$

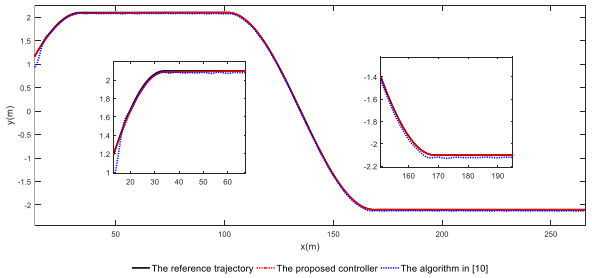


**FIGURE 3.** Position tracking of USV.

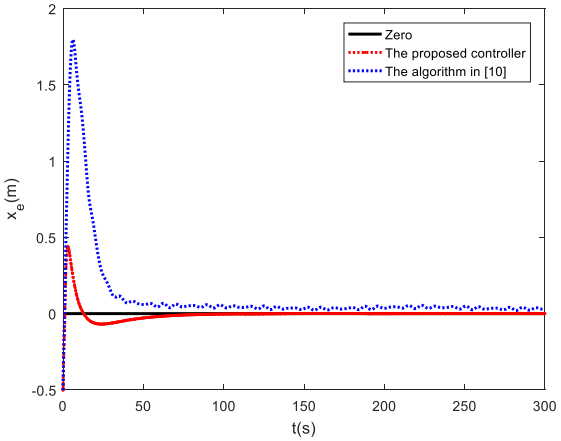


**FIGURE 4.** Position tracking errors $x_e$.

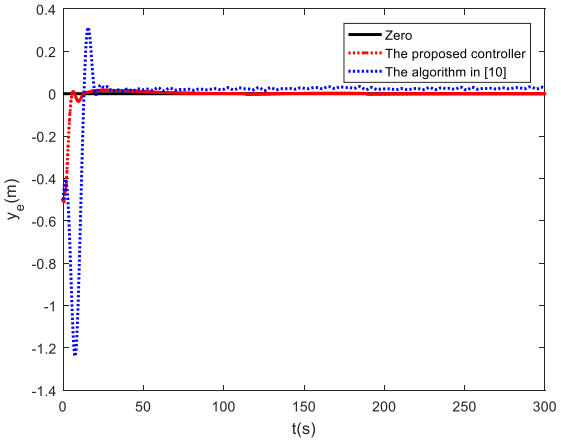


**FIGURE 5.** Position tracking errors $y_e$.

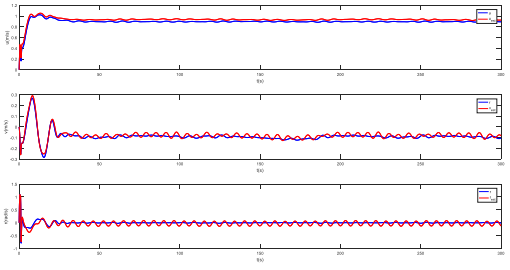

**FIGURE 6.** Real and estimated velocities.

The control parameters are chosen as follows: $c = 0.01$, $\lambda_1 = 1$, $\lambda_2 = 2$, $\lambda_3 = 2$, $\mu_r = 5$, $\mu_u = 5$, $\alpha_1 = 30$, $\alpha_2 = 50$, $\alpha_3 = 20$. The STA observer parameters are selected

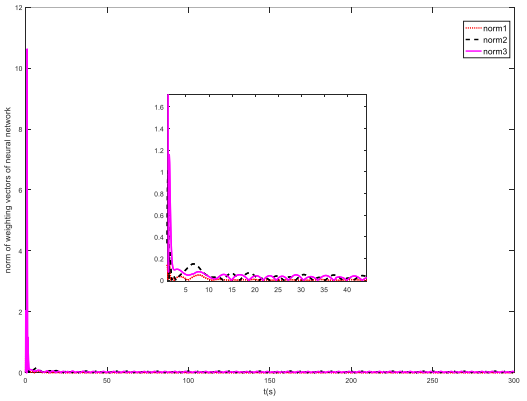


**FIGURE 7.** The norms of the RBF neural network weights.

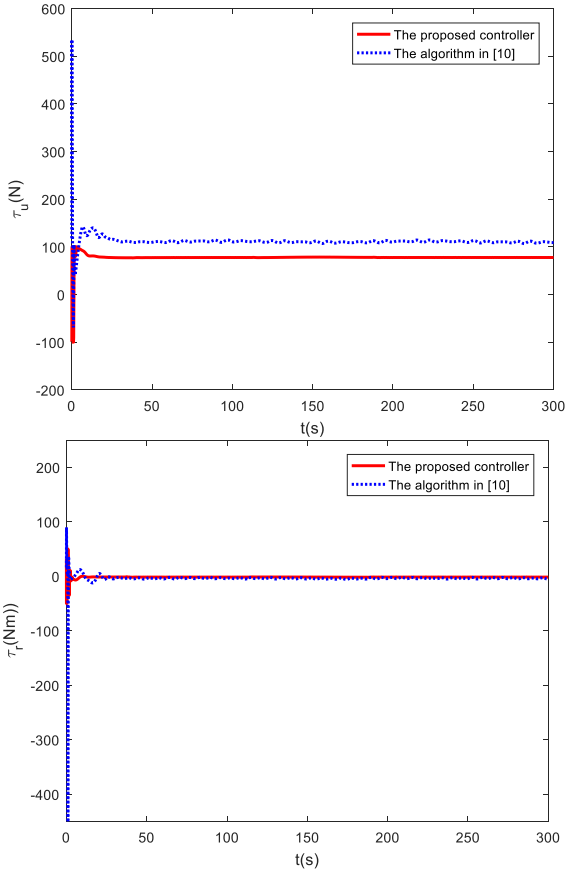


**FIGURE 8.** The USV control force and moment.

as $\lambda = 1.5$ and $\alpha = 1.1$. The predefined performance functions are chosen as follows:

$$\begin{aligned}\beta_1(t) &= (18-2)e^{-0.05t} + 2\\ \beta_2(t) &= (18-2)e^{-0.05t} + 2\\ \beta_3(t) &= (6-\pi/8)e^{-0.05t} + \pi/8\end{aligned} \tag{54}$$

Then, the parameters of the RBF NNs with six hidden nodes are chosen as $\Gamma = [15,\ 0,\ 0;\ 0,\ 20, 0; 0, 0, 45]$, $h_1 = 1$, $h_2 = 1, h_3 = 1$. The input vectors are designed as $X = [s_1, s_2, s_3, x_e, y_e, \phi_e]^T$. The width $b_j$ of the Gaussian

function is an important factor affecting the network mapping range. In the input, the closer the $c_j$ are to each other, the more sensitive the Gaussian function is. We choose appropriate values for $c_j$ according to [30], and the center vector and variances are designed using trial and error to be $b_j = 10$ and $c_j = 2[-0.2, -0.12, -0.04, 0.04, 0.12, 0.2]$.

Finally, we clearly show the advantages of the proposed controller by comparison against the algorithm used in [10], where the simulation time is set to 300 s, and the simulation results are shown in FIGUREs 3-8.

FIGURE 3 shows that the proposed method has a higher trajectory-tracking performance, as well as other advantages, compared to the algorithm in [10]. FIGURE 4 and FIGURE 5 show under the proposed controller, the tracking speed is faster and the steady-state errors are smaller than the algorithm in [10], which shows that the proposed controller has a higher dynamic performance during the initial stage of tracking and a better control effect during final stable tracking. FIGURE 6 shows that the unmeasurable velocities of USV are accurately estimated by the STA observer. The norms of the RBF NNs weights are shown in FIGURE 7. Finally, FIGURE 8 clearly shows that the control force and torque are continuous and smooth.

## VI. CONCLUSION

In this paper, a trajectory-tracking controller is proposed for underactuated surface vehicles, considering uncertainties and unmeasurable velocities. The proposed USV controller has the following advantages. (i) The system uncertainties are estimated by RBF neural networks. (ii) The unmeasurable velocities are estimated by a super-twisting observer. (iii) The position tracking error and heading-angle tracking error are guaranteed to converge using the backstepping method and a predefined performance function. Finally, the simulation results show that the proposed controller can stably and quickly track the desired trajectory when the model parameters of the USV are uncertain.

## REFERENCES

[1] C. Zhou, S. Gu, Y. Wen, Z. Du, C. Xiao, L. Huang, and M. Zhu, "The review unmanned surface vehicle path planning: Based on multi-modality constraint," *Ocean Eng.*, vol. 200, Mar. 2020, Art. no. 107043.

[2] J. Ghommam, L. Iftekhar, and M. Saad, "Adaptive finite time path-following control of underactuated surface vehicle with collision avoidance," *J. Dyn. Syst., Meas., Control*, vol. 141, no. 12, Dec. 2019, Art. no. e121008.

[3] C. Liu, R. R. Negenborn, X. Chu, and H. Zheng, "Predictive path following based on adaptive line-of-sight for underactuated autonomous surface vessels," *J. Mar. Sci. Technol.*, vol. 23, no. 3, pp. 483–494, Sep. 2018.

[4] L. Li, K. Dong, and G. Guo, "Trajectory tracking control of underactuated surface vessel with full state constraints," *Asian J. Control*, vol. 23, no. 4, pp. 1762–1771, Jul. 2021.

[5] K. D. von Ellenrieder, "Dynamic surface control of trajectory tracking Marine vehicles with actuator magnitude and rate limits," *Automatica*, vol. 105, pp. 433–442, Jul. 2019.

[6] H. Liu, G. Chen, and X. Tian, "Cooperative formation control for multiple surface vessels based on barrier Lyapunov function and self-structuring neural networks," *Ocean Eng.*, vol. 216, Nov. 2020, Art. no. 108163.

[7] G. Xia, X. Xia, B. Zhao, C. Sun, and X. Sun, "Distributed tracking control for connectivity-preserving and collision-avoiding formation tracking of underactuated surface vessels with input saturation," *Appl. Sci.*, vol. 10, no. 10, p. 3372, May 2020.

[8] Z. Dong, L. Wan, Y. Li, T. Liu, and G. Zhang, "Trajectory tracking control of underactuated USV based on modified backstepping approach," *Int. J. Nav. Archit. Ocean Eng.*, vol. 7, no. 5, pp. 817–832, Sep. 2015.

[9] C. Zhang, C. Wang, Y. Wei, and J. Wang, "Neural-based command filtered backstepping control for trajectory tracking of underactuated autonomous surface vehicles," *IEEE Access*, vol. 8, pp. 42481–42490, 2020.

[10] Z. Kai, Z. Yulong, and L. Zhaoqing, "Trajectory tracking control of underactuated unmanned surface vehicles with disturbance observer," *Ship Sci. Technol.*, vol. 41, no. 12, pp. 127–133, 2019.

[11] S. Ullah, Q. Khan, A. Mehmood, and R. Akmeliawati, "Integral backstepping based robust integral sliding mode control of underactuated nonlinear electromechanical systems," *J. Control Eng. Appl. Informat.*, vol. 21, no. 3, pp. 42–50, 2019.

[12] S. Ullah, A. Mehmood, Q. Khan, S. Rehman, and J. Iqbal, "Robust integral sliding mode control design for stability enhancement of under-actuated quadcopter," *Int. J. Control, Autom. Syst.*, vol. 18, no. 7, pp. 1671–1678, Jul. 2020.

[13] M. Li, T. Li, X. Gao, Q. Shan, C. L. P. Chen, and Y. Xiao, "Adaptive NN event-triggered control for path following of underactuated vessels with finite-time convergence," *Neurocomputing*, vol. 379, pp. 203–213, Feb. 2020.

[14] Z. Zwierzewicz, "Robust and adaptive path-following control of an underactuated ship," *IEEE Access*, vol. 8, pp. 120198–120207, 2020.

[15] Z. Sun, G. Zhang, J. Yang, and W. Zhang, "Research on the sliding mode control for underactuated surface vessels via parameter estimation," *Nonlinear Dyn.*, vol. 91, no. 2, pp. 1163–1175, Jan. 2018.

[16] K. Shojaei, "Observer-based neural adaptive formation control of autonomous surface vessels with limited torque," *Robot. Auto. Syst.*, vol. 78, pp. 83–96, Apr. 2016.

[17] X. Sun, G. Wang, and Y. Fan, "Model identification and trajectory tracking control for vector propulsion unmanned surface vehicles," *Electronics*, vol. 9, no. 1, p. 22, Dec. 2019.

[18] S. Li, J. Liu, R. R. Negenborn, and Q. Wu, "Automatic docking for underactuated ships based on multi-objective nonlinear model predictive control," *IEEE Access*, vol. 8, pp. 70044–70057, 2020.

[19] R.-C. Roman, R.-E. Precup, and E. M. Petriu, "Hybrid data-driven fuzzy active disturbance rejection control for tower crane systems," *Eur. J. Control*, vol. 58, pp. 373–387, Mar. 2021.

[20] R.-E. Precup, R.-C. Roman, T.-A. Teban, A. Albu, E. M. Petriu, and C. Pozna, "Model-free control of finger dynamics in prosthetic hand myoelectric-based control systems," *Stud. Informat. Control*, vol. 29, no. 4, pp. 399–410, Dec. 2020.

[21] S. Ullah, Q. Khan, A. Mehmood, S. A. M. Kirmani, and O. Mechali, "Neuro-adaptive fast integral terminal sliding mode control design with variable gain robust exact differentiator for under-actuated quadcopter UAV," *ISA Trans.*, Mar. 2021, doi: 10.1016/j.isatra.2021.02.045.

[22] M. Van, "An enhanced tracking control of Marine surface vessels based on adaptive integral sliding mode control and disturbance observer," *ISA Trans.*, vol. 90, pp. 30–40, Jul. 2019.

[23] Y. Deng, X. Zhang, N. Im, G. Zhang, and Q. Zhang, "Model-based event-triggered tracking control of underactuated surface vessels with minimum learning parameters," *IEEE Trans. Neural Netw. Learn. Syst.*, vol. 31, no. 10, pp. 4001–4014, Oct. 2020.

[24] M. Fu, T. Wang, and C. Wang, "Adaptive neural-based finite-time trajectory tracking control for underactuated Marine surface vessels with position error constraint," *IEEE Access*, vol. 7, pp. 16309–16322, 2019.

[25] B. S. Park and S. J. Yoo, "Robust fault–tolerant tracking with predefined performance for underactuated surface vessels," *Ocean Eng.*, vol. 115, pp. 159–167, Mar. 2016.

[26] S. L. Dai, S. He, and H. Lin, "Transverse function control with prescribed performance guarantees for underactuated Marine surface vehicles," *Int. J. Robust Nonlinear Control*, vol. 29, no. 5, pp. 1577–1596, 2019.

[27] Z. Zheng, L. Ruan, M. Zhu, and X. Guo, "Reinforcement learning control for underactuated surface vessel with output error constraints and uncertainties," *Neurocomputing*, vol. 399, pp. 479–490, Jul. 2020.

[28] K. D. Do and J. Pan, "Global tracking control of underactuated ships with nonzero off-diagonal terms in their system matrices," *Automatica*, vol. 41, no. 1, pp. 87–95, Jan. 2005.

[29] L. Chen, R. Cui, C. Yang, and W. Yan, "Adaptive neural network control of underactuated surface vessels with guaranteed transient performance: Theory and experimental results," *IEEE Trans. Ind. Electron.*, vol. 67, no. 5, pp. 4024–4035, May 2020.
[30] B. S. Park, J.-W. Kwon, and H. Kim, "Neural network-based output feedback control for reference tracking of underactuated surface vessels," *Automatica*, vol. 77, pp. 353–359, Mar. 2017.
[31] Z. Jia, Z. Hu, and W. Zhang, "Adaptive output-feedback control with prescribed performance for trajectory tracking of underactuated surface vessels," *ISA Trans.*, vol. 95, pp. 18–26, May 2019.
[32] C. Zhang, C. Wang, J. Wang, and C. Li, "Neuro-adaptive trajectory tracking control of underactuated autonomous surface vehicles with high-gain observer," *Appl. Ocean Res.*, vol. 97, Apr. 2020, Art. no. 102051.
[33] H. Liu and H. K. Khalil, "Output feedback stabilization using super-twisting control and high-gain observer," *Int. J. Robust Nonlinear Control*, vol. 29, no. 3, pp. 601–617, 2019.
[34] H. N. Esfahani, R. Szlapczynski, and H. Ghaemi, "High performance super-twisting sliding mode control for a maritime autonomous surface ship (MASS) using ADP-based adaptive gains and time delay estimation," *Ocean Eng.*, vol. 191, Nov. 2019, Art. no. 106526.
[35] M. Morawiec and A. Lewicki, "Speed observer structure of induction machine based on sliding super-twisting and backstepping techniques," *IEEE Trans. Ind. Informat.*, vol. 17, no. 2, pp. 1122–1131, Feb. 2021.
[36] R. Cui, L. Chen, C. Yang, and M. Chen, "Extended state observer-based integral sliding mode control for an underwater robot with unknown disturbances and uncertain nonlinearities," *IEEE Trans. Ind. Electron.*, vol. 64, no. 8, pp. 6785–6795, Aug. 2017.
[37] A. Turnip and H. J. Panggabean, "Hybrid controller design based magneto-rheological damper lookup table for quarter car suspension," *Int. J. Artif. Intell.*, vol. 18, no. 1, pp. 193–206, Mar. 2020.
[38] R. Yang, Y. Yu, J. Sun, and H. R. Karimi, "Event-based networked predictive control for networked control systems subject to two-channel delays," *Inf. Sci.*, vol. 524, pp. 136–147, Jul. 2020.
[39] N. Wang and H. Li, "Leader-follower formation control of surface vehicles: A fixed-time control approach," *ISA Trans.*, May 2020, doi: 10.1016/j.isatra.2020.05.042.
[40] J. Zhang, S. Yu, and Y. Yan, "Fixed-time extended state observer-based trajectory tracking and point stabilization control for Marine surface vessels with uncertainties and disturbances," *Ocean Eng.*, vol. 186, Aug. 2019, Art. no. 106109.
[41] Z. Shen, Y. Wang, H. Yu, and C. Guo, "Finite-time adaptive tracking control of Marine vehicles with complex unknowns and input saturation," *Ocean Eng.*, vol. 198, Feb. 2020, Art. no. 106980.
[42] H. Liu and G. Chen, "Robust trajectory tracking control of Marine surface vessels with uncertain disturbances and input saturations," *Nonlinear Dyn.*, vol. 100, no. 4, pp. 3513–3528, Jun. 2020.
[43] C. Liu, Z. Zou, and J. Yin, "Trajectory tracking of underactuated surface vessels based on neural network and hierarchical sliding mode," *J. Mar. Sci. Technol.*, vol. 20, no. 2, pp. 322–330, Jun. 2015.
[44] J. Davila, L. M. Fridman, and A. Levant, "Second-order sliding-mode observer for mechanical systems," *IEEE Trans. Autom. Control*, vol. 50, no. 11, pp. 1785–1789, Nov. 2005.
[45] S.-L. Dai, S. He, M. Wang, and C. Yuan, "Adaptive neural control of underactuated surface vessels with prescribed performance guarantees," *IEEE Trans. Neural Netw. Learn. Syst.*, vol. 30, no. 12, pp. 3686–3698, Dec. 2019.

**LANPING ZOU** received the B.E. degree from Tianjin University of Technology and Education, Tianjin, China, in 2015. She is currently pursuing the master's degree with the School of Mechanical and Power Engineering, Guangdong Ocean University. Her research interests include sliding mode control and robust adaptive control.

**HAITAO LIU** received the Ph.D. degree from the School of Mechanical and Automotive Engineering, South China University of Technology, Guangzhou, China, in 2012. He is currently a Professor with the School of Mechanical and Power Engineering, Guangdong Ocean University, Zhanjiang, China. His current research interests include the theory and applications of nonlinear control and robotics.

**XUEHONG TIAN** received the B.Sc. degree in engineering management and the M.E. degree in mechanical engineering from Guangdong Ocean University, Zhanjiang, China, in 2011 and 2018, respectively. She is currently an Assistant Researcher at Guangdong Ocean University. Her research interests include robot control, multi-agent systems, and nonlinear systems design.